Published in final edited form as:
Dev Dyn. 2011 August ; 240(8): 1964–1976. doi:10.1002/dvdy.22680.

Aberrant expression of genes necessary for neuronal development and Notch signaling in an epileptic *mind bomb* zebrafish

Gabriela A. Hortopan[1] and **Scott C. Baraban**[1,*]

[1]Epilepsy Research Laboratory, Department of Neurological Surgery, University of California, San Francisco, San Francisco, California 94143.

Abstract

Mutation within an ubiquitin E3 ligase gene can lead to a failure in Notch signaling, excessive neurons, and depletion of neural progenitor cells in *mind bomb* mutants. Using *mib*^{hi904} zebrafish, we reported seizures and a down-regulation of GABA signaling pathway genes. A transcriptome analysis also identified differential expression pattern of genes related to Notch signaling and neurodevelopment. Here we selected nine of these genes (her4.2, hes5, bhlhb5, hoxa5a, hoxb5b, dmbx1a, dbx1a, nxph1 and plxnd1) and performed a more thorough analysis of expression using conventional polymerase chain reaction, real-time polymerase chain reaction and in situ hybridization. Transgenic reporter fish (Gfap:GFP and Dlx5a-6a:GFP) were used to assess early brain morphology in vivo. Down-regulation of many of these genes was prominent throughout key structures of the developing *mib*^{hi904} zebrafish brain including, but not limited to, the pallium, ventral thalamus, and optic tectum. Brain expression of Dlx5a-6a and Gfap was also reduced. In conclusion, these expression studies indicate a general down-regulation of Notch signaling genes necessary for proper brain development and suggest that these mutant fish could provide valuable insights into neurological conditions, such as Angelman syndrome, associated with ubiquitin E3 ligase mutation.

Keywords

brain; development; GFP; Notch; zebrafish

INTRODUCTION

Notch signaling plays an essential role in early brain development including, but not limited to, cell fate determination (Dontu et al., 2004), pattern formation (Lewis et al., 2009), neurogenesis and gliogenesis (Jülich et al., 2005; Taylor et al., 2007; Wheeler et al., 2008; Xiao et al., 2009). Membrane-bound Notch is proteolyzed by TNFα-converting enzyme, metalloproteases and presenilin into an active form that is translocated to the nucleus where it forms a complex with CSL (CBF1/RBP-Jκ, Su(H), Lag-1) (Jarriault et al., 1995; Lu et al., 1996). This complex is a transcriptional activator triggering expression of downstream target genes such as Hairy/Enhancer-of-split (*Hes*), which inhibit basic helix-loop-helix transcription factors with additional roles in neurodevelopment (Lecourtois and Schweisguth, 1998; Mumm and Kopan, 2000; Bailey and Posakony, 1995; Hirata et al., 2002a; Holley et al., 2002a; Oates and Ho, 2002b).

*Correspondence to: Scott C. Baraban, Department of Neurological Surgery, University of California, San Francisco, Box 0112, 513 Parnassus Avenue, San Francisco, CA 94143. scott.baraban@ucsf.edu..

Mutagenesis screens in zebrafish have identified several mutants of the Notch signaling pathway: *after eight (aei)* (*delta D*), *deadly seven (des)* (*notch 1a*), *beamter (bea)* (*delta C*) and *mind bomb (mib)*(Jiang et al., 1996a; vanEeden et al., 1996a). Loss-of-function mutations in zebrafish display a so-called "neurogenic" phenotype, marked by overproduction of primary neurons early in development and a later reduction in secondary neurons. The mutation identified in *mib*^{hi904} zebrafish disrupts a conserved putative E3 ubiquitin ligase regulating Notch signaling (Golling et al. 2002a; Chen and Corliss, 2004b). Ubiquitin ligases which contain substrate-binding domains providing critical elements for specificity of target proteins or catalytic domains (such as HECT and RING fingers), comprise one of the largest families of enzymes in human cells, and have been linked to multiple human diseases. For example, the human neurogenetic disorder, Angelman syndrome (AS), can be caused by loss-of-function mutations in E3 ubiquitin ligase (*ube3a*) (Kishino et al., 1997). Phenotypic hallmarks of AS include motor dysfunction leading to an ataxic gait, frequent severe seizures, profound learning disability, absent speech, and characteristic happy demeanor (Lossie et al., 2001). Mouse models of AS exhibit an increased incidence of seizures, poor performance on Rotarod assays, and defects in long-term potentiation (Jiang et al., 1998; Miura et al., 2002). We recently showed that a *mib*^{hi904} E3 ubiquitin ligase mutant zebrafish exhibits electrographic and behavioral seizure activity (Hortopan et al. 2010). A transcriptome analysis of *mib*^{hi904} zebrafish, at three days post-fertilization (dpf), identified differential expression of GABA signaling pathway and neurodevelopmental (Notch signaling pathway related) genes (Hortopan et al. 2010). In the previous manuscript, we focused on analysis of GABA signaling genes as these may directly underlie the observed epileptic phenotype. Here we examined expression of a group of microarray-identified neurodevelopment genes in the central nervous system of *mib*^{hi904} zebrafish at 3 dpf e.g., a larval time point when these mutants exhibit a severe neurogenic phenotype and epilepsy. Confocal analysis of early brain development using live GFP reporter fish (Gfap:GFP and Dlx5/6:GFP) was also performed.

RESULTS

A transcriptome analysis using an Affymetrix zebrafish microarray containing 16,416 genes was recently performed on *mib*^{hi904} mutants (homozygotes) and age-matched sibling controls at 3 dpf (Hortopan et al. 2010). Microarray data was validated using conventional reverse transcriptase-polymerase chain reaction (RT-PCR) and real-time quantitative PCR (qPCR) for nine genes with putative roles in neurodevelopment (Table 1; Fig. 1). To further define the expression of these genes, we completed in situ hybridization studies using whole-mount larvae and cryostat sections through the central nervous system. Results of these studies are presented in detail below.

Hairy-related 4.2 (*her4.2*) and **hairy/enhancer of split 5 (*hes5*)**, Notch responsive basic helix-loop-helix genes (Takke and Campos-Ortega, 1999; Kawamura et al., 2005; Bae et al., 2005; Hegde et al., 2008b), show a significant 4-fold microarray and 3-fold real-time qPCR decrease in *mib*^{hi904} zebrafish consistent with prior observations in *mib*^{ta52b} mutants (Hwang et al., 2009b). A lateral view of the head, in whole-mount in situ hybridization (WISH), for WT control zebrafish revealed prominent *her4.2* mRNA expression in forebrain, midbrain and hindbrain (Fig. 2A). Transverse cryostat sections showed a more detailed expression pattern of *her4.2* in telencephalon, especially in the large pallial domain and continued posteriorly into subpallium through the anterior commissure (Fig. 2A1). In diencephalon, strongly homogenous clusters of *her4.2* cells can be found along the midline in dorsal (Fig. 2A2) and ventral thalamus (Fig. 2A3). Caudal to pallium, *her4.2* expression appears in the eminentia thalami and preoptic region (Figs. 2A2-A3). Metencephalon (midbrain) displays strong and extensive *her4.2* expression in the ventral region of posterior tuberculum and in the intermediate and caudal hypothalamus (Figs. 2A4-A5). Still at

midbrain level, more posteriorly in the mesencephalon, *her4.2* expression is prominent down the midline and as a band along the optic tectum and tegmentum boundary (Figs. 2A4-A5). In contrast, *her4.2* WISH expression is dramatically reduced in age-matched *mib*^{hi904} mutants and detectable only in sparsely distributed clusters throughout the CNS. A lateral WISH view, shows only a few small clusters of *her4.2* cells in subpallium and pallium (compare Figs. 2B and 2A). Transverse cryostat sections of the forebrain clearly demonstrate the presence of only small clusters of *her4.2* expression in pretectum, dorsal region of the posterior tuberculum and anterior commissure (Fig. 2B1). Diencephalon displays diffuse small clusters of *her2.4* expression in dorsal thalamus and in the lateral forebrain bundle (Figs. 2B2-B3). In optic tectum, medial, basal and lateral small clusters of *her2.4* can be seen throughout the three transverse cryostat sections (Figs. 2B3-B5), together with small *her2.4* expressing cell clusters located in the ventral region of posterior tuberculum (Figs. 2B4-B5) and hypothalamus (Fig. 2B4). Midline expression was strongly reduced in *mib*^{hi904} mutants and no detectable expression was noted in the retina.

A similar, though somewhat less prominent, pattern of WISH expression was found for *hes5*. Of interest in WT controls, a distinct pattern of *hes5* expression, with a predominant accumulation in forebrain and midbrain, was observed (Fig. 3A). In cryostat sections through telencephalon, pallium and subpallium, *hes5* expression appears near the ventricular surface (Fig. 3A1). In diencephalon, *hes5* signal continues into the optic tectum (Figs. 3A2-A4), eminentia thalami and preoptic region (Figs. 3A1-A2) as well as the ventral portion of posterior tuberculum and intermediate hypothalamus (Fig. 3A3). Strong *hes5* expression was noted near the tectal ventricle, torus semicircularis and rostral region of medulla oblongata (Fig. 3A4). “Blobs” of *hes5* expression in caudal hypothalamus are also present. As described above for *her4.2*, strong *hes5* expression is seen in the retina of WT zebrafish (Fig. 3A1) but not age-matched *mib*^{hi904} mutants; WISH also revealed a cluster of *hes5* expression primarily restricted to midbrain (Fig. 3B). Transverse sections show *hes5*-expressing aggregates corresponding to early migrating cells in the pre-tectum (Figs. 3B1-B2) that fail to extend down into thalamus and hypothalamus (Figs. 3B3-B4).

Class B5 (*bhlhb5*), a basic helix-loop-helix domain containing transcription factor (Brunelli et al., 2003), exhibited a 5-fold down-regulation in microarray and almost 3-fold down-regulation in qPCR in *mib*^{hi904} mutants compared to controls. Lateral and dorsal WISH views in WT controls revealed prominent *bhlhb5* expression at the forebrain and midbrain-hindbrain boundary (Figs. 4 A-B). Strong forebrain expression is also present in the olfactory pits, as noted in transverse and coronal sections (Figs. 4A1, 4Ci). Although only faint diencephalic *bhlhb5* expression appears in transverse sections (Fig. 4A2), *bhlhb5* can be seen clearly in dorsal views and coronal sections (Fig. 4C, Ci). More posteriorly in optic tectum, approximately at the level of the tectal ventricle, *bhlhb5* expression becomes even stronger (Fig. 4A3). In addition, *bhlhb5* is expressed in the WT eye where it is normally distributed into retinal nuclear layers. It has been shown that targeted deletion of Bhlhb5 causes loss of GABA-producing amacrine and Type 2 OFF-cone bipolar cells (Feng et al., 2006; Dulin et al., 2007). Considering the crucial role of Bhlhb5 in the specification of both cell subtypes, this could explain why expression is more diffuse in the *mib*^{hi904} mutant eye where the retinal layers do not appear to differentiate (Figs. 4B2 and 4Di). Also, in *mind bomb* mutants, there is no detectable *bhlhb5* expression in the olfactory pits (Figs. 4B, B1, D) and only faint or weak expression in diencephalon (dorsal thalamus) (Figs. 4B2-3).

Hoxa5a, hoxb5b* and *dmbx1a, homeobox genes with roles in embryonic hindbrain patterning and brain development (Holland and Takahashi, 2005), exhibit a nearly 2-fold down-regulation in *mib*^{hi904} mutants compared to controls. WISH revealed remarkable WT expression patterns at rhombomere boundaries and lower expression in pharyngeal arches 6 and 7 for *hoxa5a* and *hoxb5b* genes (Figs. 5A, 5B, 5E, 5F), in agreement with previous

studies (McGinnis and Krumlauf, 1992; Krumlauf, 1994, Davis and Stellwag, 2010). However, in *mib*^{hi904} mutants there is no detectable *hoxa5a* expression in hindbrain (Figs. 5C-D) and only small collections of *hoxb5b* at rhombomere boundaries and in pharyngeal arches (Figs. 5G-H). In WT, *dmbx1a* was expressed robustly throughout midbrain and hindbrain (Fig. 6A). Transverse sections revealed prominent clusters of *dmbx1a* expression in optic tectum and retina (Figs. 6A1-A2). In midbrain, *dmbx1a* clusters were noted at the level of the cerebellum, in the cerebellar commissure and torus semicircularis (Fig. 6A3) and posteriorly reaching the medulla oblongata (Fig. 6A). In contrast, *dmbx1a* expression is barely detectable in *mib*^{hi904} mutants (Fig. 6B); only few *dmbx1a*-expressing cell clusters are visible in optic tectum, retina (Figs. 6B1-B3) and the midbrain-hindbrain boundary (Fig. 6B).

Another related homeobox gene (Fjose et al., 1994), ***dbx1a***, exhibited 2-fold up-regulation in microarray and almost 2-fold up-regulation in qPCR in *mib*^{hi904} mutants. In WT, WISH revealed *dbx1a* expression in forebrain, continuing through midbrain and ending at the hindbrain-medulla oblongata boundary (Fig. 7A). Transverse sections show discrete domains of *dbx1a* in the pallium (Fig. 7A1) and similar clusters of expression in dorsal thalamus (Fig. 7A2), optic tectum and pretectum (Fig. 7A2-A3). Caudal to the pallium, *dbx1a* expression appears in the eminentia thalami (Fig. 7A3); a small number of *dbx1a*-expressing cells can be seen in rostral hypothalamus (Fig. 7A4) and cerebellum (Fig. 7A5). WISH in *mib*^{hi904} mutant revealed a greater degree of *dbx1a* expression following the same distribution profile seen in WT siblings (Fig. 7B). In transverse sections, a dense strip of pallial *dbx1a* expression was observed in diencephalon and a very prominent expression pattern was noted in optic tectum, pretectum and dorsal thalamus (Fig. 7B1) extending posteriorly (Figs. 7B2-B3). In diencephalon, some *dbx1a*-expressing cells were observed in the eminentia thalami (Fig. 7B3). More caudally, *dbx1a* expression extends dorsally reaching cerebellum and posteriorly into the medulla oblongata (Figs. 7B4-B5). There is no detectable *dbx1a* expression in hypothalamus of *mib*^{hi904} mutants.

Plexin D1, a receptor for the semaphorin family of ligands with a crucial role in regulating axonal pathfinding, neuronal patterning (Tamagnone and Comoglio, 2000) and patterning of developing blood vessels (Torres-Vazquez et al., 2004), exhibited a 3-fold up-regulation in microarray and nearly 2-fold in qPCR. WISH shows faint *plxnd1* expressed only at the level of the branchial arches in WT siblings (Fig. 8A). In sharp contrast, *mib*^{hi904} mutants show an aberrant increase in *plxnd1* expression concentrated to the forebrain, optic tectum and branchial arches (Fig. 8B). In contrast, **neurexophilin 1** (*nxph1*), a family of neuropeptide-like secreted glycoproteins (Petrenko et al., 1996), appeared to have the opposite pattern of expression to Plexin D1 in *mib*^{hi904} *mutants*. WISH revealed clusters of *nxph1* expression in forebrain, midbrain and hindbrain in WT (Fig. 9A). In transverse sections, much of this *nxph1* expression is restricted to the pallium region (telencephalon) and some glomerular structures within the habenula and dorsal thalamus (Fig. 9A1). Caudal to pallium, *nxph1* expression appears in eminentia thalami (Fig. 9A2), ventral thalamus, through the posterior tuberculum (Fig. 9A2) and rostral hypothalamus (Fig. 9A3). *Nxph1* expression appears heterogeneous in optic tectum and smaller scattered clusters were noted in medulla oblongata (Fig. 9A); *nxph1* is barely detected around the branchial arches and medulla oblongata in *mib*^{hi904} mutants at 3 dpf (Fig. 9B, 9B1-9B3).

GFP expression in live zebrafish

Glial fibrillary acidic protein (Gfap) is a member of the intermediate filament family of proteins found in astroglial cells and early neuronal progenitors. Consistent with previous studies (Hegde et al., 2008b), Gfap expression appeared to be 6-fold down-regulated in microarray and almost 4-fold in qPCR in *mib*^{hi904} mutants. To further assess in vivo expression using confocal microscopy, a transgenic line of zebrafish expressing a green

fluorescent protein driven by Gfap specific regulatory elements (Gfap:GFP tg) was crossed into the *mib*^{hi904} background. In confocal images from anesthetized and immobilized WT siblings, Gfap drove expression (shown as green fluorescence) in telencephalon, retina and midbrain and was prominent in hindbrain and spinal cord (Figs. 10A-B). A distinctly different and more diffuse expression pattern was observed in *mib*^{hi904} mutants, where reduced Gfap-GFP fluorescence was observed in optic tectum and retina. Although more GFP fluorescence was spread posteriorly in hindbrain and medulla oblongata (compared to optic tectum), overall GFP fluorescence in *mib*^{hi904} mutants was diffuse and notably less than in WT controls (Figs. 10C-D).

The eight distal-less (Dlx) genes present in zebrafish (Ekker, Akimenko et al. 1992; Akimenko, Ekker et al. 1994) encode a family of transcription factors involved in the formation of the forebrain, branchial arches, pharyngeal dentition, sensory organs, and limbs (Zerucha et al., 2000; Park et al., 2004; Borday-Birraux et al., 2006; Burton, 2008; MacDonald et al., 2010a). Anesthetized and immobilized, 3 dpf WT larvae show GFP expression in the telencephalon, diencephalon and optic tectum, but also in some groups of cells in the cerebellar region (Figs. 10E-F) consistent with previous reports in transgenic zebrafish at 5 dpf (Mione et al., 2008). Only few cells in diencephalon and cerebellum (Figs. 10G-H) express Dlx5a-6a in *mib*^{hi904} mutants.

DISCUSSION

Zebrafish *mind bomb* mutants are characterized by a severe neurogenic phenotype with defects somite, neural crest, and vasculature development. These defects have been interpreted as a consequence of abnormal Notch signaling (Jiang et al., 1996a; Lawson et al., 2001; Schier et al., 1996; van Eeden et al., 1996a; Haddon et al., 1998a; Riley et al., 1999). For example, early in development, Notch target genes such as basic Helix–Loop–Helix (*bhlh*) or Hairy/Enhancer of Split (*hes*) are up-regulated in critical areas of the central nervous system (Bray and Furriols, 2001) and these, in turn, suppress transcription of proneural genes such as neurogenin which prevents neighboring cells from adopting a neuronal fate in a process called “lateral inhibition” (Camposortega, 1995). Disruption of E3 ubiquitin ligase activity in *mind bomb* mutants leads to a failure in Notch signaling, resulting in a down-regulation of *bhlh* and *hes* genes, an excess of early differentiating neurons, a deficit of late differentiating neurons, impaired lateral inhibition (Schier et al., 1996; Jiang et al., 1996a; Itoh et al., 2003; Park and Appel, 2003; Yeo and Chitnis, 2007) and a striking disorganization of all regions of the CNS (Golling et al., 2002a). Decreased Notch activity is also suggested by reports of reduced expression of the transcriptional repressor *her4* gene and increased expression of *neurogenin-1* (Chen and Corliss, 2004b; Hegde et al., 2008b; Hwang et al., 2009b). Here down-regulation in *her4* and two additional Notch pathway genes (*hes5* and *bhlhb5*) were confirmed in telencephalon, metencephalon and optic tectum of *mib*^{hi904} mutants at 3 dpf. Hairy-related and hairy/enhancer of split genes were previously shown to be down-regulated in microarray studies on *mib*^{ta52b} mutants (Hwang et al., 2009), but these studies did not examine spatial expression patterns in the CNS. That these Notch signaling genes show decreased expression along the midline, a proliferative zone in the larval zebrafish brain (Mueller and Wullimann, 2005), further suggests a critical role for E3 ubiquitin ligase in mediating neuronal differentiation.

Expression of a proneural bHLH gene (*bhlhb5*) required for forebrain organization and co-expressed in regions along the midline where Dlx genes (i.e., transcription factors required for the tangential migration of GABAergic interneurons during brain development; Anderson et al., 1997) have been reported (Mueller and Wullimann, 2005) was nearly below detectable levels in *mib*^{hi904} mutants. Not surprisingly, loss of neurodevelopmental gene expression in this region of the developing brain ultimately leads to a disruption of forebrain

cytoarchitecture and marked reductions in both GABAergic interneuron markers (Hortopan et al., 2009) and Dlx5/6-expressing interneurons (Fig. 10). At a functional level, neuronal disorganization and reduced interneuron density are likely contributors to the observed epileptic phenotype in *mib*^{hi904} mutants. Interestingly, expression of multiple members of the *bhlh* family of transcription factors (Lee, 1997; Bramblet et al., 2002; McLellan et al., 2002; Xu et al., 2002) are also differentially regulated following chemically induced status epilepticus in rats (Elliott et al., 2001). Given that *bhlh* genes show similar expression changes in an epileptic *mib*^{hi904} mutant and in zebrafish CNS structures shown to generate abnormal electrical activity e.g., optic tectum and telencephalon (Hortopan et al. 2010), suggests they might be functionally related to epileptogenesis.

Dramatically reduced *mib*^{hi904} mutant expression of homeobox (*hoxa5a* and *hoxb5b*) genes was also noted. *Hox* genes act as super-regulators of development and are often simultaneously expressed in tissue where they activate or repress transcription of multiple downstream target genes involved in morphogenesis, segmental specification and neurodevelopment (Gilbert, 2000; Kawahara et al., 2002). Both *hoxa5a* and *hoxb5b* show almost negligible expression in forebrain structures sub-serving higher brain functions such as the telencephalon and optic tectum; *dmbx1a* expression was robust throughout midbrain and hindbrain of control fish but nearly absent from *mib*^{hi904} mutants. In contrast, one up-regulated homeobox gene (*dbx1a*) was heavily over-expressed in the ventral forebrain and hindbrain. Recent studies in *dbx1* mutant mice indicate that homeodomain transcription factors act upstream of Notch signaling, and it is believed that homeodomain proteins control spatial distribution of Notch ligands and proteins (Marklund et al., 2010). Using software that predicts interaction partners for one protein within a specific species and *dbx1* as an example, we also noted a strong association between *hes5*, *dmbx1a* and *dbx1a*. COGs (Clusters of Orthologous Groups of proteins) are very powerful and can help identify direct (physical) and indirect (functional) associations between genes. These *in silica* analyses support our qPCR findings, where we found a high Pearson correlation between the corresponding genes (Supplemental Table 1). To better illustrate these correlations and interactions, 3D graphs were created using relative expression values from qPCR. One example is shown in Supplemental Fig. 1, where *dbx1a* expression, shown to be up-regulated in the microarray assay in *mib*^{hi904} mutants (B), is plotted with two other down-regulated genes, *her4.2* and *nxph1*. The pattern observed in WT zebrafish (A) is opposite; these last two genes, *her4.2* and *nxph1*, increase their expression while the *dbx1a* drops down (inversely correlated). A different pattern of response was observed when the same gene, *dbx1a*, was plotted with other two genes, *plxnd1* and *hes5*, in WT (C) and in *mib*^{hi904} mutants (D). This would be the first step for the definition of a model to predict co-variation gene expression patterns and for the use of some of these genes (molecular markers) as a potential diagnostic tool.

Notch signaling is also involved in vascular development (Jakobsson et al., 2009; Roca and Adams, 2007) and vascular defects in the trunk of three different Notch zebrafish mutants were recently described (Therapontos and Vargesson, 2010). Although these studies focused on trunk vascularization, expression of *plxnd1* in the head of these mutants was also reported and is similar to the pattern of expression we observed in *mib*^{hi904} mutants. Interestingly, *nxph1*, expressed in discrete clusters in the habenula, pallium, and ventral thalamus of control fish (but nearly absent in the forebrain and midbrain of *mib*^{hi904} mutants) functions as an endogenous ligand for α-neurexins (Missler and Sudhof, 1998d). Neurexins, together with neuroligins, are thought to play an essential role in synaptic transmission, particularly at GABAergic synapses (Craig and Kang, 2007). This is consistent with our recent demonstration (Hortopan et al. 2010) that GABA signaling may be reduced in *mind bomb* mutants presumably contributing to defective inhibitory synaptic transmission and epilepsy. Finally, neurexin-ligand interactions are also important for development and/or maturation

of synaptic connections (Clarris et al., 2002) and implicated in the pathophysiology of neurodevelopmental disorders e.g., neurexin-1 was recently associated with autism (Ching et al., 2010a) a co-morbidity noted in children with Angelman syndrome.

When *mib*^{hi904} mutants were crossed with transgenic reporter lines (Gfap:GFP or Dlx5/6:GFP) a strong general down-regulation in fluorescence was noted. For glial fibrillary acidic protein, this is consistent with microarray and qPCR data (Hortopan et al. 2010) and previous independent analysis of the spinal cord (Song et al., 2010b). Mutations in human *gfap* have been described in association with a severe childhood brain disorder i.e., Alexander disorder (Brenner et al., 2001; Quinlan et al., 2007) characterized by enlarged brain and head size, seizures, stiffness in the arms/legs, intellectual disability, and developmental delay. Dlx5a-6a:GFP transgenic zebrafish provide a means to further study GABAergic interneurons (Mione et al., 2008; MacDonald et al., 2010b). Confocal images of *mib*^{hi904} zebrafish mutants crossed into this reporter line show a clear decrease of cells in forebrain and midbrain, suggestive of a failure in the differentiation or migration of early born interneurons. Although deficits in cell density could be a contributing factor to gene expression patterns seen throughout this manuscript, general brain morphology as indicated by these in vivo GFP imaging studies suggests that major CNS structures are largely intact in *mib*^{hi904} mutants.

In conclusion, altered expression levels and patterns in *mib*^{hi904} mutants of genes critical to early stages of neurodevelopment support the view that an ubiquitin E3 ligase is involved in Notch signaling. In contrast to earlier studies of *mind bomb* zebrafish mutants focused on development of the pituitary gland (Dutta et al., 2008), hindbrain (Bingham et al., 2003), spinal cord (Itoh et al., 2003) or mesoderm (Hwang et al., 2009), our studies focused on gene expression patterns in critical regions of the zebrafish telencephalon and metencephalon. Failure or reduction in ligase activity in these regions can, as shown here, lead to down-regulation of several Notch signaling genes that are required for normal neuronal development. Loss of this signaling led to dramatic alterations in how the brain develops with potentially catastrophic consequences for inhibitory synapse formation, cognitive function, and survival (*mib* mutants do not survive past 4 dpf). Although this study only represents a relatively small subset of neurodevelopmental genes that may be disturbed, it is possible that *mib*^{hi904} mutants could help to characterize mechanisms that underlie symptoms of disorders that require proper development of synaptic circuits.

EXPERIMENTAL PROCEDURES

Animals and maintenance

Heterozygote zebrafish (*mind bomb*, line #hi904) were obtained from the Zebrafish International Resource Center (Eugene, OR; http://zebrafish.org/zirc/fish/lineAll.php). The following transgenic lines were also used in this study: Gfap:GFP (*Tg(gfap:GFP)*$^{mi2001/+}$; Chen et al. 2010) and Dlx5a-6a:GFP (Zerucha et al., 2000). Adult zebrafish were maintained according to standard procedures (Westerfield, 1993), and following guidelines approved by the University of California, San Francisco Institutional Animal Care and Use Committee. Zebrafish embryos and larvae were maintained in egg water (0.03% Instant Ocean).

RNA isolation

At 3 dpf, larvae were sorted by morphology and used for RNA isolation. Total RNA was isolated from 14 pools of larvae (4 fish/pool): mib mutants (n = 7) and age-matched WT sibling controls (n = 7). Fish were treated with Trizol® Reagent (Invitrogen, Carlsbad, CA), RNase-free DNase to remove possible genomic DNA contamination, and quantified with GeneQuant® spectrophotometer.

PCR, cloning and sequencing

cDNA was generated using a mix of random primers and oligo(dT)20 in a reverse transcription kit (SuperScript™III First-Strand Synthesis System, Invitrogen) according to the manufacturer's protocol. Primers pairs, forward and reverse, were specifically designed using Primer 3 web software (http://frodo.wi.mit.edu/primer3/) for each investigated gene (Supplemental Table 2). The most conserved regions were identified by sequence alignment (ClustalW, Thompson et al., 1994) of all available gene sequences from GeneBank including other fish species. We used BLAST software to investigate primer cross-specificity and Mfold software (Zuker, 2003) to check for secondary structure of the entire DNA sequence. Each reaction cycle (32 loops) consisted of incubations at 94°C (30 sec), 60°C (30 sec), and 72°C (60 sec) with Taq DNA Polymerase (Taq PCR Core kit, Qiagen). A 2% agarose gel electrophoresis stained with ethidium bromide was used to separate PCR products which were further cloned in pCR®II-TOPO® plasmid vector (TOPO TA Cloning System, Invitrogen) according to the manufacturer's specifications. DNA sequencing was performed by Elim Biopharmaceuticals, Inc. (Hayward, CA).

Quantitative real-time PCR (qPCR)

Gene expression levels were determined by real-time qPCR using SybrGreen® fluorescent master mix on an ABI Prism® 7700 Sequence Detection System driven by ABI prism SDS v9.1 software (Applied Biosystems). The cDNA templates were diluted 1:2 with DEPC (diethyl pyrocarbonate) sterile water before qPCR applications to minimize the presence of potential inhibitors. Primer Express v3.0 software (Applied Biosystems) was used to design all primers on our own sequenced cDNA to produce amplicons ranging in size between 71bp to 125bp (Supplemental Table 3) and then synthesized by Invitrogen. Samples were run in triplicate in 10 μL of 1× SYBR green master mix containing 100 nM of each primer and RNAse free water. Samples without reverse transcriptase and samples without RNAs were run for each reaction as negative controls. Cycling parameters were as follows: 50°C × 2min, 95°C × 10min, then 45 cycles of the following 95°C × 15s, 60°C × 1min. For each sample a dissociation step was performed at 95°C × 15s, 60°C × 20s and 95°C × 15 s. Dissociation (melting) curve analysis showed no sign of primer-dimers or other non-specific reaction products.

For qPCR data, significant differences were considered at P value ≤ 0.05 (Student's t test). Relative quantification of the target gene transcript with β-actin reference gene transcript (Hortopan et al., 2010) was made following both the Comparative ΔΔCT (Livak and Schmittgen, 2001) and the Efficiency Based (Pfaffl, 2001) methods using qCalculator software (programmed by Ralf Gilsbach, Institute of Pharmacology and Toxicology, University of Bonn, Germany), which also estimates qPCR efficiency E= 10(– 1/slope). Similar results were obtained with both types of analyses. Standard curves for all nine genes, to estimate qPCR efficiencies, were constructed using a 4-fold serial dilution of pooled cDNA; 5 standards assayed in triplicate: 1/1; 1/4; 1/16; 1/64; 1/256 (the efficiencies, slope of the curves and the correlation coefficient are summarized in Supplemental Table 3).

Whole-mount in situ hybridization (WISH)

Antisense and sense RNA probes were generated from plasmids corresponding to each of the 9 selected genes using specific restriction enzymes for linearization (New England Biolabs, UK). Linearized DNA template (1 μg) was purified (QIAquick®, Qiagen) and incubated for 3 hour at 37°C in a solution containing 10X transcription buffer, dithiothreitol (DTT; 100mM), 10X Dig NTP Mix (Roche), RNAse inhibitor (20U/μl), and RNA polymerase (20U/μl) T7 or SP6. After digestion of the DNA template with DNase (10U/μl) for 15 minutes at 37°C and incubation, the product was purified using a mix of RNAse-free water and LiCl (30 μl, 1:2) and left overnight at -20°C. After centrifugation at 4°C and

washing with 70% ethanol (RNAse free), the pellet was dried and stored in hybridization mix solution at -20°C until use.

3dpf embryos, mib mutants (n = 8) and WT controls (n = 8) for each antisense and sense RNA probes, were sorted and fixed in 4% paraformaldehyde (PFA) then stored in 100% methanol at -20°C. Following storage at -20°C, fixed larvae were rehydrated in a series of methanol and PBS-0.1%Tween20 (PBST) washes. Whole-mount in situ hybridization was performed as previously described (Hauptmann and Gerster, 1994). Larvae were fixed in 4% PFA, washed in PBST and processed for cryo-sectioning using quick-frozen samples mounted in O.C.T. compound (Tissue TEK®; slice thickness: 15-20 μm).

Transgenic zebrafish

Transgenic Gfap:GFP zebrafish (*Tg(gfap:GFP)*$^{mi2001/+}$) founder lines were obtained from the Zebrafish International Research Center (http://zebrafish.org/zirc/home/guide.php). Adult GFP founder lines on an AB background were crossed with heterozygote *mind bomb* (*mib*$^{hi904Tg/+}$) founders on an AB background. F1 fish were sorted by fluorescence as embryos, raised to adulthood and crossed to obtain mib:Gfap:GFP larvae. 30 fish larvae were sorted at 3 dpf, (mib; n = 15 and WT; n = 15) and anesthetized in a cocktail containing 0.02% Tricaine and α-bungarotoxin (1 mg/ml) or curare (4.5 mM), then immersed in 1.2% low melting point agarose to immobilize and orientate the embryos for imaging. Visual assessment of GFP expression was performed using a Leica SP5 confocal scanning fluorescence microscope. Confocal images were reconstructed using z-stack projections produced from serial scanning every 4 μm.

Microscopy and imaging

Tissue sections of larval zebrafish were chosen to be representative of gene expression and matched, as well as possible, with respect to location and cutting angle. WISH figures are annotated to show the approximate location and cutting angle for each section. Pictures of whole-mount in situ hybridization embryos mounted in 70% glycerol and slide-mounted cryosections were taken using a Zeiss Axioskop microscope equipped with a computer-controlled Optronics MicroFire camera system. Raw images were imported into Adobe Photoshop and slightly adjusted for contrast and sharpness.

Terminology

Neuroanatomical designations were taken from Mueller and Wullimann (2005) in consultation with Thomas Mueller.

Supplementary Material

Refer to Web version on PubMed Central for supplementary material.

Acknowledgments

We would like to thank Matthew Dinday and Thomas Mueller for their valuable contributions to this manuscript. This work was supported by funds from the National Institutes of Health (R01 NS053479-03) to S.C.B.

Grant sponsor: NIH; Grant number: NS053479-03

REFERENCES

Akimenko MA, Ekker M, Wegner J, Lin W, Westerfield M. Combinatorial expression of 3 zebrafish genes related to distal-less - part of a homeobox gene code for the head. J Neurosci. 1994; 14:3475–3486. [PubMed: 7911517]

Anderson SA, Eisenstat DD, Shi L, Rubenstein JL. Interneuron migration from basal forebrain to neocortex: dependence on Dlx genes. Science. 1997; 278:474–476. [PubMed: 9334308]

Bae YK, Shimizu T, Hibi M. Patterning of proneuronal and inter-proneuronal domains by hairy- and enhancer of split-related genes in zebraf ish neuroectoderm. Development. 2005; 132:1375–1385. [PubMed: 15716337]

Bailey AM, Posakony JW. Suppressor of hairless directly activates transcription of enhancer of split complex genes in response to notch receptor activity. Gene Dev. 1995; 9:2609–2622. [PubMed: 7590239]

Biehlmaier O, Neuhauss SCF, Kohler K. Onset and time course of apoptosis in the developing retina of zebrafish. Invest Ophth Vis Sci. 2001; 42:3407.

Bingham S, Chaudhari S, Vanderlaan G, Itoh M, Chitnis A, Chandrasekhar A. Neurogenic phenotype of mind bomb mutant leads to severe patterning defects in the zebrafish hindbrain. Dev Dynam. 2003; 228:451–463.

Borday-Birraux V, Van der Heyden C, Debiais-Thibaud M, Verreijdt L, Stock DW, Huysseune A, Sire JY. Expression of Dlx genes during the development of the zebrafish pharyngeal dentition: evolutionary implications. Evol Dev. 2006; 8:130–141. [PubMed: 16509892]

Bramblett DE, Copeland NG, Jenkins NA, Tsai MJ. BHLHB4 is a bHLH transcriptional regulator in pancreas and brain that marks the dimesencephalic boundary. Genomics. 2002; 79:402–412. [PubMed: 11863370]

Bray S, Furriols M. Notch pathway: Making sense of suppressor of hairless. Curr Biol. 2001; 11:R217–R221. [PubMed: 11301266]

Brenner M, Johnson AB, Boespflug-Tanguy O, Rodriguez D, Goldman JE, Messing A. Mutations in GFAP, encoding glial fibrillary acidic protein, are associated with Alexander disease. Nat Genet. 2001; 27:117–120. [PubMed: 11138011]

Brunelli S, Innocenzi A, Cossu G. Bhlhb5 is expressed in the CNS and sensory organs during mouse embryonic development. Gene Expr Patterns. 2003; 3:755–759. [PubMed: 14643684]

Burton, L. M.Sc. thesis, University of Ottawa MR48591. 2008. Dlx regulation in zebrafish brain development via I56i/I56ii and I12a/I12b..

Camposortega JA. Genetic mechanisms of early neurogenesis in Drosophila-melanogaster. Mol Neurobiol. 1995; 10:75–89.

Chen HL, Yuh CH, Wu KK. Nestin Is Essential for Zebrafish Brain and Eye Development through Control of Progenitor Cell Apoptosis. Plos One. 2010:5.

Chen WB, Corliss DC. Three modules of zebrafish Mind bomb work cooperatively to promote Delta ubiquitination and endocytosis. Dev Biol. 2004b; 267:361–373. [PubMed: 15013799]

Ching MSL, Shen YP, Tan WH, Jeste SS, Morrow EM, Chen XL, Mukaddes NM, Yoo SY, Hanson E, Hundley R, Austin C, Becker RE, Berry GT, Driscoll K, Engle EC, Friedman S, Gusella JF, Hisama FM, Irons MB, Lafiosca T, LeClair E, Miller DT, Neessen M, Picker JD, Rappaport L, Rooney CM, Sarco DP, Stoler JM, Walsh CA, Wolff RR, Zhang T, Nasir RH, Wu BL, Childrens Hosp Boston Genotype P. Deletions of NRXN1 (Neurexin-1) Predispose to a Wide Spectrum of Developmental Disorders. Am J Med Genet B. 2010a; 153B:937–947.

Clarris HJ, McKeown S, Key B. Expression of neurexin ligands, the neuroligins and the neurexophilins, in the developing and adult rodent olfactory bulb. Int J Dev Biol. 2002; 46:649–652. [PubMed: 12141453]

Craig AM, Kang Y. Neurexin-neuroligin signaling in synapse development. Curr Opin Neurobiol. 2007; 17:43–52. [PubMed: 17275284]

Davis A, Stellwag EJ. Spatio-temporal patterns of Hox paralog group 3-6 gene expression during Japanese medaka (Oryzias latipes) embryonic development. Gene Expr Patterns. 2010; 10:244–250. [PubMed: 20471497]

Dontu G, Jackson KW, McNicholas E, Kawamura MJ, Abdallah WM, Wicha MS. Role of Notch signaling in cell-fate determination of human mammary stem/progenitor cells. Breast Cancer Res. 2004; 6:R605–R615. [PubMed: 15535842]

Dulin JP, Locker M, Robach M, Henningfeld KA, Parain K, Afelik S, Pieler T, Perron M. Ptf1a triggers GABAergic neuronal cell fates in the retina. BMC Dev Biol. 2007; 7:110. [PubMed: 17910758]

Dutta S, Dietrich J- E, Westerfield M, Varga ZM. Notch signaling regulates endocrine cell specification in the zebrafish anterior pituitary. Dev Biol. 2008; 319:248–257. [PubMed: 18534570]

Ekker M, Akimenko MA, Bremiller R, Westerfield M. Regional expression of 3 homeobox transcripts in the inner-ear of zebrafish embryos. Neuron. 1992; 9:27–35. [PubMed: 1352984]

Elliott RC, Khademi S, Pleasure SJ, Parent JM, Lowenstein DH. Differential regulation of basic helix-loop-helix mRNAs in the dentate gyrus following status epilepticus. Neuroscience. 2001; 106:79–88. [PubMed: 11564418]

Fjose A, Izpisuabelmonte JC, Fromentalramain C, Duboule D. Expression of the zebrafish gene hlx-1 in the prechordal plate and during cns development. Development. 1994; 120:71–81. [PubMed: 7907015]

Feng L, Xie X, Joshi PS, Yang Z, Shibasaki K, Chow RL, Gan L. Requirement for Bhlhb5 in the specification of amacrine and cone bipolar subtypes in mouse retina. Development. 2006; 133:4815–25. [PubMed: 17092954]

Gavrieli Y, Sherman Y, Bensasson SA. Identification of programmed cell-death insitu via specific labeling of nuclear-dna fragmentation. J Cell Biol. 1992; 119:493–501. Development 2006, 133:4815-25. [PubMed: 1400587]

Gilbert S, F. Developmental biology, 6th edition. Sinauer Associates; Sunderland, Mass.: 2000.

Golling G, Amsterdam A, Sun ZX, Antonelli M, Maldonado E, Chen WB, Burgess S, Haldi M, Artzt K, Farrington S, Lin SY, Nissen RM, Hopkins N. Insertional mutagenesis in zebrafish rapidly identifies genes essential for early vertebrate development. Nat Genet. 2002a; 31:135–140. [PubMed: 12006978]

Haddon C, Jiang YJ, Smithers L, Lewis J. Delta-Notch signalling and the patterning of sensory cell differentiation in the zebrafish ear: evidence from the mind bomb mutant. Development. 1998a; 125:4637–4644. [PubMed: 9806913]

Hauptmann G, Gerster T. Two-color whole-mount in-situ hybridization to vertebrate and drosophila embryos. Trends Genet. 1994; 10:266–266. [PubMed: 7940754]

Hegde A, Qiu NC, Qiu XH, Ho SHK, Tay KQY, George J, Ng FSL, Govindarajan KR, Gong ZY, Mathavan S, Jiang YJ. Genomewide Expression Analysis in Zebrafish mind bomb Alleles with Pancreas Defects of Different Severity Identifies Putative Notch Responsive Genes. Plos One. 2008b:3.

Hirata H, Yoshiura S, Ohtsuka T, Bessho Y, Harada T, Yoshikawa K, Kageyama R. Oscillatory expression of the bHLH factor Hes1 regulated by a negative feedback loop. Science. 2002a; 298:840–843. [PubMed: 12399594]

Hjorth JT, Key B. Are pioneer axons guided by regulatory gene expression domains in the zebrafish forebrain? High-resolution analysis of the patterning of the zebrafish brain during axon tract formation. Dev Biol. 2001; 229:271–286. [PubMed: 11203695]

Holland PWH, Takahashi T. The evolution of homeobox genes: Implications for the study of brain development. Brain Res Bull. 2005; 66:484–490. [PubMed: 16144637]

Holley SA, Julich D, Rauch GJ, Geisler R, Nusslein-Volhard C. her1 and the notch pathway function within the oscillator mechanism that regulates zebrafish somitogenesis. Development. 2002; 129:1175–1183. [PubMed: 11874913]

Hortopan GA, Dinday MT, Baraban SC. Spontaneous Seizures and Altered Gene Expression in GABA Signaling Pathways in a mind bomb Mutant Zebrafish. J Neurosci. 2010; 30:13718–13728. [PubMed: 20943912]

Hwang J, Kim HS, Seok JW, Kim JD, Koun S, Park SY, Lee J, Kim KS, Chang KT, Ryoo ZY, Wang SM, Huh TL, Lee S. Transcriptome analysis of the zebrafish mind bomb mutant. Mol Genet Genomics. 2009b; 281:77–85. [PubMed: 19005681]

Itoh M, Kim CH, Palardy G, Oda T, Jiang YJ, Maust D, Yeo SY, Lorick K, Wright GJ, Ariza-McNaughton L, Weissman AM, Lewis J, Chandrasekharappa SC, Chitnis AB. Mind bomb is a ubiquitin ligase that is essential for efficient activation of Notch signaling by delta. Dev Cell. 2003; 4:67–82. [PubMed: 12530964]

Jakobsson L, Bentley K, Gerhardt H. VEGFRs and Notch: a dynamic collaboration in vascular patterning. Biochem Soc T. 2009; 37:1233–1236.

Jarriault S, Brou C, Logeat F, Schroeter EH, Kopan R, Israel A. Signaling downstream of activated mammalian notch. Nature. 1995; 377:355–358. [PubMed: 7566092]

Jiang YH, Armstrong D, Albrecht U, Atkins CM, Noebels JL, Eichele G, Sweatt JD, Beaudet AL. Mutation of the angelman ubiquitin ligase in mice causes increased cytoplasmic p53 and deficits of contextual learning and long-term potentiation. Neuron. 1998; 21:799–811. [PubMed: 9808466]

Jiang YJ, Brand M, Heisenberg CP, Beuchle D, FurutaniSeiki M, Kelsh RN, Warga RM, Granato M, Haffter P, Hammerschmidt M, Kane DA, Mullins MC, Odenthal J, vanEeden FJM, NussleinVolhard C. Mutations affecting neurogenesis and brain morphology in the zebrafish, Danio rerio. Development. 1996a; 123:205–216. [PubMed: 9007241]

Julich D, Lim CH, Round J, Nicolaije C, Schroeder J, Davies A, Geisler R, Lewis J, Jiang YJ, Holley SA, Tubingen Screen C. beamter/deltaC and the role of Notch ligands in the zebrafish somite segmentation, hindbrain neurogenesis and hypochord differentiation. Dev Biol. 2005; 286:391–404. [PubMed: 16125692]

Kawahara A, Chien CB, Dawid IB. The homeobox gene mbx is involved in eye and tectum development. Dev Biol. 2002; 248:107–117. [PubMed: 12142024]

Kawamura A, Koshida S, Hijikata H, Sakaguchi T, Kondoh H, Takada S. Zebrafish hairy/enhancer of split protein links FGF signaling to cyclic gene expression in the periodic segmentation of somites. Gene Dev. 2005; 19:1156–1161. [PubMed: 15905406]

Kishino T, Lalande M, Wagstaff J. UBE3A/E6-AP mutations cause Angelman syndrome (vol 15, pg 70, 1997). Nat Genet. 1997; 15:411–411.

Krumlauf R. Hox genes in vertebrate development. Cell. 1994; 78:191–201. [PubMed: 7913880]

Lawson ND, Scheer N, Pham VN, Kim CH, Chitnis AB, Campos-Ortega JA, Weinstein BM. Notch signaling is required for arterial-venous differentiation during embryonic vascular development. Development. 2001; 128:3675–3683. [PubMed: 11585794]

Lecourtois M, Schweisguth F. Indirect evidence for Delta-dependent intracellular processing of notch in Drosophila embryos. Curr Biol. 1998; 8:771–774. [PubMed: 9651681]

Lee JE. Basic helix-loop-helix genes in neural development. Curr Opin Neurobiol. 1997; 7:13–20. [PubMed: 9039799]

Lewis J, Hanisch A, Holder M. Notch signaling, the segmentation clock, and the patterning of vertebrate somites. J Biol (London). 2009:8.

Livak KJ, Schmittgen TD. Analysis of relative gene expression data using real-time quantitative PCR and the 2(T)(-Delta Delta C) method. Methods. 2001; 25:402–408. [PubMed: 11846609]

Lossie AC, Whitney MM, Amidon D, Dong HJ, Chen P, Theriaque D, Hutson A, Nicholls RD, Zori RT, Williams CA, Driscoll DJ. Distinct phenotypes distinguish the molecular classes of Angelman syndrome. J Med Genet. 2001; 38:834–845. [PubMed: 11748306]

Lu FM, Lux SE. Constitutively active human Notch1 binds to the transcription factor CBF1 and stimulates transcription through a promoter containing a CBF1-responsive element. P Natl Acad Sci Usa. 1996; 93:5663–5667.

MacDonald RB, Debiais-Thibaud M, Ekker M. Regulation of Dlx gene expression in the zebrafish pharyngeal arches: from conserved enhancer sequences to conserved activity. J Appl Ichthyol. 2010a; 26:187–191.

MacDonald RB, Debiais-Thibaud M, Talbot JC, Ekker M. The Relationship Between dlx and gad1 Expression Indicates Highly Conserved Genetic Pathways in the Zebrafish Forebrain. Dev Dynam. 2010b; 239:2298–2306.

Marklund U, Hansson EM, Sundstrom E, de Angelis MH, Przemeck GKH, Lendahl U, Muhr J, Ericson J. Domain-specific control of neurogenesis achieved through patterned regulation of Notch ligand expression. Development. 2010; 137:437–445. [PubMed: 20081190]

McGinnis W, Krumlauf R. Homeobox genes and axial patterning. Cell. 1992; 68:283–302. [PubMed: 1346368]

McLellan AS, Langlands K, Kealey T. Exhaustive identification of human class II basic helix-loop-helix proteins by virtual library screening. Gene Expr Patterns. 2002; 2:329–335. [PubMed: 12617822]

Mione M, Baldessari D, Deflorian G, Nappo G, Santoriello C. How neuronal migration contributes to the morphogenesis of the CNS: Insights from the zebrafish. Dev Neurosci-Basel. 2008; 30:65–81.

Missler M, Sudhof TC. Neurexophilins form a conserved family of neuropeptide-like glycoproteins. J Neurosci. 1998d; 18:3630–3638. [PubMed: 9570794]

Miura K, Kishino T, Li E, Webber H, Dikkes P, Holmes GL, Wagstaff J. Neurobehavioral and electroencephalographic abnormalities in Ube3a maternal-deficient mice. Neurobiol Dis. 2002; 9:149–159. [PubMed: 11895368]

Mueller, T.; Wullimann, MF. Atlas of early zebrafish brain development: A tool for molecular neurogenetics, 1st ed. Elsevier; Amsterdam: 2005. p. xip. 183

Mumm JS, Kopan R. Notch signaling: From the outside in. Dev Biol. 2000; 228:151–165. [PubMed: 11112321]

Oates AC, Ho RK. Hairy/E(spl)-related (Her) genes are central components of the segmentation oscillator and display redundancy with the Delta/Notch signaling pathway in the formation of anterior segmental boundaries in the zebrafish. Development. 2002b; 129:2929–2946. [PubMed: 12050140]

Park BK, Sperber SM, Choudhury A, Ghanem N, Hatch GT, Sharpe PT, Thomas BL, Ekker M. Intergenic enhancers with distinct activities regulate Dlx gene expression in the mesenchyme of the branchial arches. Dev Biol. 2004; 268:532–545. [PubMed: 15063187]

Park HC, Appel B. Delta-Notch signaling regulates oligodendrocyte specification. Development. 2003; 130:3747–3755. [PubMed: 12835391]

Petrenko AG, Ullrich B, Missler M, Krasnoperov V, Rosahl TW, Sudhof TC. Structure and evolution of neurexophilin. Journal of Neuroscience. 1996; 16:4360–4369. [PubMed: 8699246]

Pfaffl MW. A new mathematical model for relative quantification in real-time RT-PCR. Nucleic Acids Res. 2001:29. [PubMed: 11125041]

Quinlan RA, Brenner M, Goldman JE, Messing A. GFAP and its role in Alexander disease. Exp Cell Res. 2007; 313:2077–2087. [PubMed: 17498694]

Riley BB, Chiang MY, Farmer L, Heck R. The deltaA gene of zebrafish mediates lateral inhibition of hair cells in the inner ear and is regulated by pax2.1. Development. 1999; 126:5669–5678. [PubMed: 10572043]

Roca C, Adams RH. Regulation of vascular morphogenesis by Notch signaling. Gene Dev. 2007; 21:2511–2524. [PubMed: 17938237]

Schier AF, Neuhauss SCF, Harvey M, Malicki J, SolnicaKrezel L, Stainier DYR, Zwartkruis F, Abdelilah S, Stemple DL, Rangini Z, Yang H, Driever W. Mutations affecting the development of the embryonic zebrafish brain. Development. 1996; 123:165–178. [PubMed: 9007238]

Song YQ, Willer JR, Scherer PC, Panzer JA, Kugath A, Skordalakes E, Gregg RG, Willer GB, Balice-Gordon RJ. Neural and Synaptic Defects in slytherin, a Zebrafish Model for Human Congenital Disorders of Glycosylation. Plos One. 2010b:5.

Takke C, Campos-Ortega JA. her1, a zebrafish pair-rule like gene, acts downstream of notch signalling to control somite development. Development. 1999; 126:3005–3014. [PubMed: 10357943]

Tamagnone L, Comoglio PM. Signalling by semaphorin receptors: cell guidance and beyond. Trends Cell Biol. 2000; 10:377–383. [PubMed: 10932095]

Taylor MK, Yeager K, Morrison SJ. Physiological Notch signaling promotes gliogenesis in the developing peripheral and central nervous systems. Development. 2007; 134:2435–2447. [PubMed: 17537790]

Therapontos C, Vargesson N. Zebrafish Notch Signalling Pathway Mutants Exhibit Trunk Vessel Patterning Anomalies That Are Secondary to Somite Misregulation. Dev Dynam. 2010; 239:2761–2768.

Thompson JD, Higgins DG, Gibson TJ. Clustal-W - improving the sensitivity of progressive multiple sequence alignment through sequence weighting, position-specific gap penalties and weight matrix choice. Nucleic Acids Res. 1994; 22:4673–4680. [PubMed: 7984417]

Torres-Vazquez J, Gitler AD, Fraser SD, Berk JD, Pham VN, Fishman MC, Childs S, Epstein JA, Weinstein BM. Semaphorin-plexin signaling guides patterning of the developing vasculature. Dev Cell. 2004; 7:117–123. [PubMed: 15239959]

vanEeden FJM, Granato M, Schach U, Brand M, FurutaniSeiki M, Haffter P, Hammerschmidt M, Heisenberg CP, Jiang YJ, Kane DA, Kelsh RN, Mullins MC, Odenthal J, Warga RM, Allende ML,

Weinberg ES, NussleinVolhard C. Mutations affecting somite formation and patterning in the zebrafish, Danio rerio. Development. 1996a; 123:153–164.

Westerfield, M. The zebrafish book: a guide for the laboratory use of zebrafish (Brachydanio rerio). University of Oregon Press; Eugene, OR: 1993.

Wheeler SR, Stagg SB, Crews ST. Multiple Notch signaling events control Drosophila CNS midline neurogenesis, gliogenesis and neuronal identity. Development. 2008; 135:3071–3079. [PubMed: 18701546]

Xiao MJ, Han Z, Shao B, Jin K. Notch signaling and neurogenesis in normal and stroke brain. Int J Physiol Pathophysiol Pharmacol. 2009; 1:192–202. [PubMed: 20428478]

Xu ZP, Dutra A, Stellrecht CM, Wu CY, Piatigorsky J, Saunders GF. Functional and structural characterization of the human gene BHLHB5, encoding a basic helix-loop-helix transcription factor. Genomics. 2002; 80:311–318. [PubMed: 12213201]

Yeo SY, Chitnis AB. Jagged-mediated Notch signaling maintains proliferating neural progenitors and regulates cell diversity in the ventral spinal cord. P Natl Acad Sci USA. 2007; 104:5913–5918.

Zerucha T, Stuhmer T, Hatch G, Park BK, Long QM, Yu GY, Gambarotta A, Schultz JR, Rubenstein JLR, Ekker M. A highly conserved enhancer in the Dlx5/Dlx6 intergenic region is the site of cross-regulatory interactions between Dlx genes in the embryonic forebrain. J Neurosci. 2000; 20:709–721. [PubMed: 10632600]

Zuker M. Mfold web server for nucleic acid folding and hybridization prediction. Nucleic Acids Res. 2003; 31:3406–3415. [PubMed: 12824337]

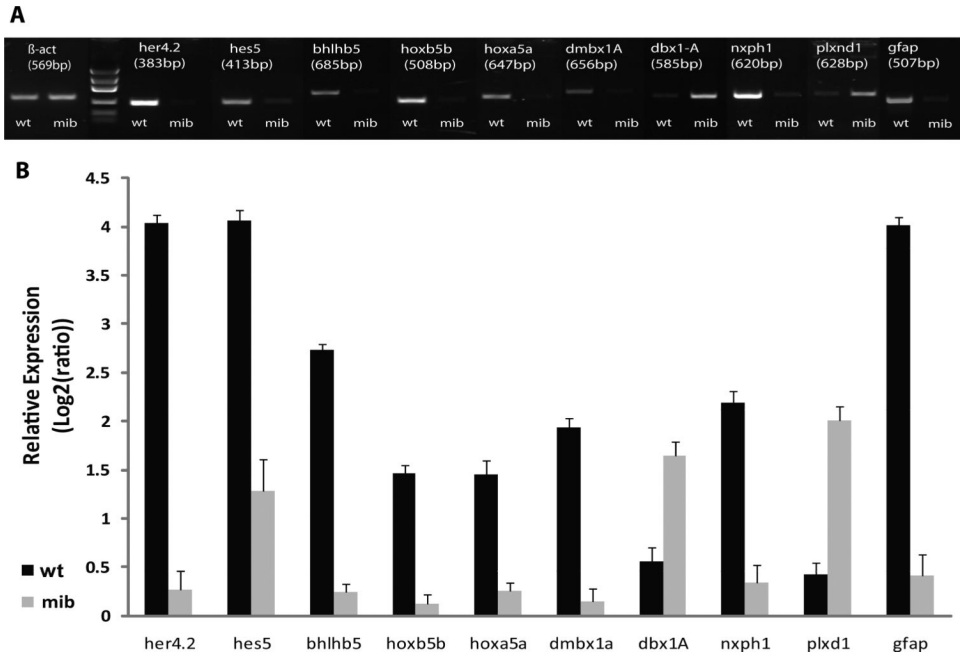

Fig.1.

Gene expression detection of all the genes of interest (*gfap* included), using (A) RT-PCR in 2% ethidium bromide agarose gel electrophoresis and (B) quantitative real-time PCR (qPCR). Levels of mRNA, measured by qPCR were normalized to β-act. Error bars indicate ± SEM. Student's t-test, $p<0.05$. Abbreviations: *bhlhb5*, basic helix-loop-helix domain containing, class B, 5; *dbx1a*, developing brain homeobox 1a; *dmbx1a*, diencephalon/ mesencephalon homeobox 1a; *gfap*, glial fibrillary acidic protein; *her4.2*, hairy-related 4.2; *hes5*, hairy and enhancer of split 5; *hoxa5a*, homeo box A5a; *hoxb5b*, homeobox protein (hoxb5b) gene; *nxph1*, neurexophilin 1; *plxnd1*, plexin D1.

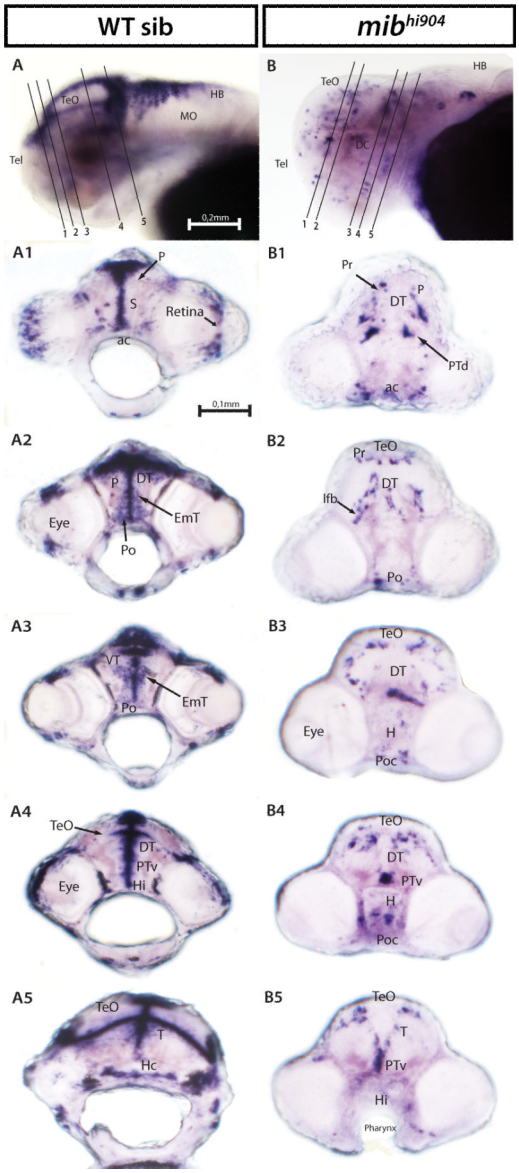

Fig. 2.

her4.2 mRNA expression in WT sibling (left panels) and *mib*^{hi904} mutant zebrafish (right panels) by in situ hybridization. Whole mounts are shown in lateral views (A, B). A1-A5: WISH transversal cryostat sections of a stage 72 hours post-fertilization (hpf) WT sibling at levels illustrated by the dashed lines in A. B1-B5: WISH transversal cryostat sections of a stage 72 hpf *mib*^{hi904} mutant at levels illustrated by the dashed lines in B. Note that dashed lines were indicatively drawn here (and in all subsequent figures) to reflect the approximate cutting angle and location. Abbreviations: ac, anterior commissure; DC, diencephalon; DT, dorsal thalamus; EmT, eminentia thalami; H, hypothalamus; HB, hindbrain; Hc, caudal hypothalamus; Hi, intermediate hypothalamus; lfb, lateral forebrain bundle; MO, medulla oblongata; P, pallium; Po, preoptic region; Poc, postoptic commissure; Pr, pretectum; PTd, dorsal part of posterior tuberculum; PTv, ventral part of posterior tuberculum; S, subpallium; T, midbrain tegmentum; Tel, telencephalon; TeO, tectum opticum; VT, ventral thalamus. Scale Bar: 0.2 mm (A, B), 0.1 mm (A1-A5, B1-B5).

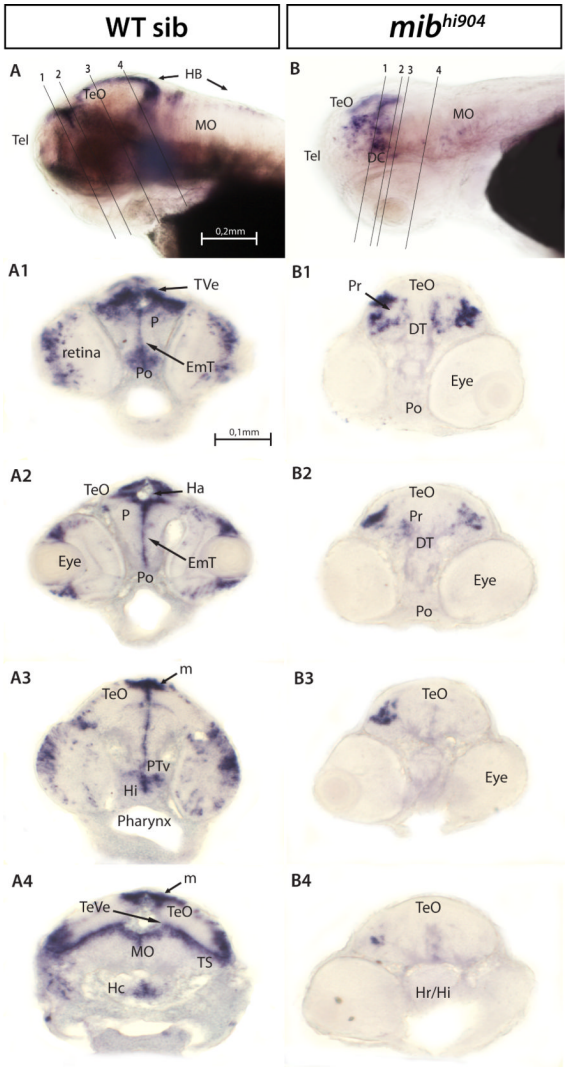

Fig. 3.

hes5 mRNA. Whole mounts are shown in lateral views (A, B). A1-A4: WISH transversal cryostat sections of a stage 72 hpf WT. B1-B4: WISH transversal cryostat sections of a stage 72hpf *mib*^{hi904}. Note that it is difficult to precisely match thin cut sections of the larval zebrafish (e.g., eye is smaller in B3 and B4) and this does not reflect an asymmetrical expression pattern in the midbrain. Abbreviations (as in A): Ha, habenula; Hr, rostral hypothalamus; m, medial tectum opticum; PTv, ventral part of posterior tuberculum; TeVe, tectal ventricle; TS, torus semicircularis; TVe, telencephalic ventricle. Scale Bar: 0.2 mm (A, B), 0.1 mm (A1-A4, B1-B4).

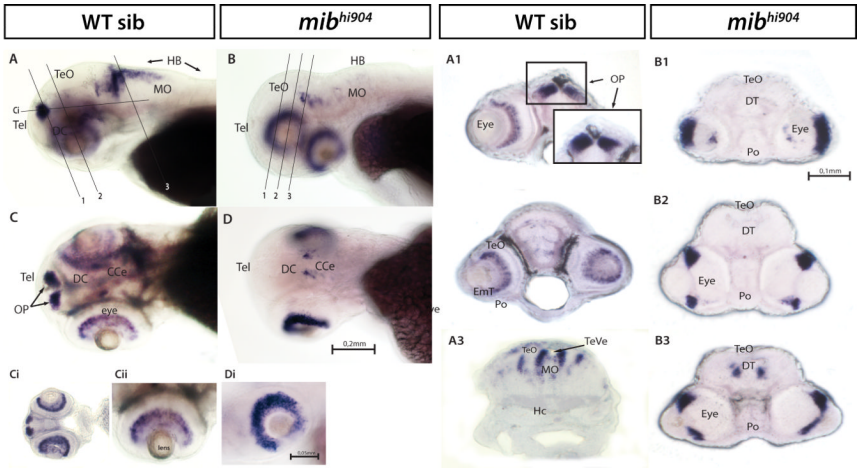

Fig. 4.

bhlhb5 mRNA expression. Whole mounts are shown in lateral (A, B) and dorsal views (C, D). Smaller panels (Ci, Di) show a higher magnification of the eye, in lateral views. Note the *mib*^{hi904} mutant eye where the retinal layers fail to differentiate. A1-A3: WISH transversal cryostat sections of a stage 72 hpf WT. A4-A5: WISH coronal cryostat sections of a stage 72 hpf WT. B1-B3: WISH transversal cryostat sections of a stage 72 hpf *mib*^{hi904} mutant. Abbreviations (as above): CCe, cerebellum; INL, inner nuclear layer; GCL, ganglion cell layer; ONL, outer nuclear Layer; OP, olfactory pits. Scale Bar: 0.2 mm (A, B, C, D), 0.1 mm (A1-A5, B1-B3), 0.05 mm (Ci, Di).

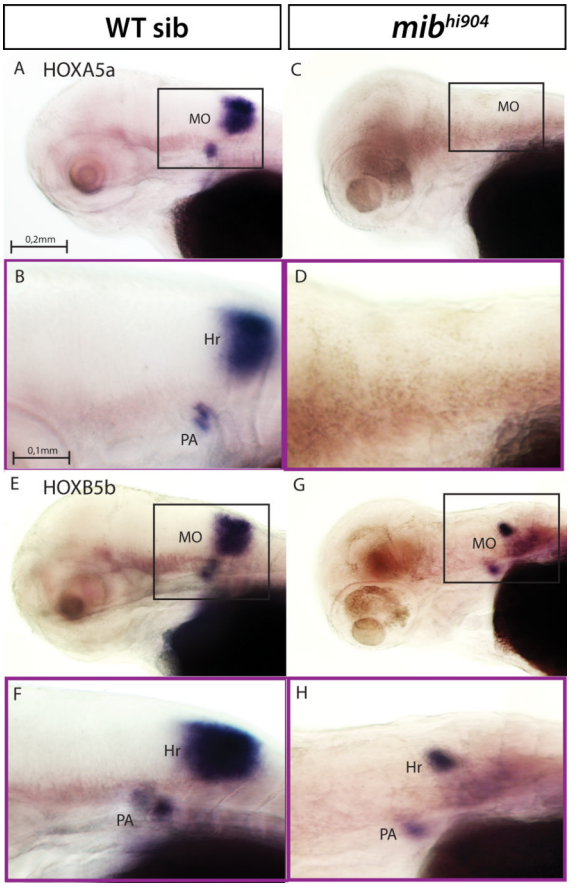

Fig. 5.

hoxa5a and *hoxb5b* mRNA expression. Upper panels (A, C, E, G) - whole mounts are shown in lateral views. Lower panels (B, D, F, H) - higher magnification and same orientation of area framed in A, C, E, G. Abbreviations (as above): Hr, hindbrain rhombomeres; PA, pharyngeal arch. Scale bars: 0.2 mm (A, C, E, G), 0.1 mm (B, D, F, H).

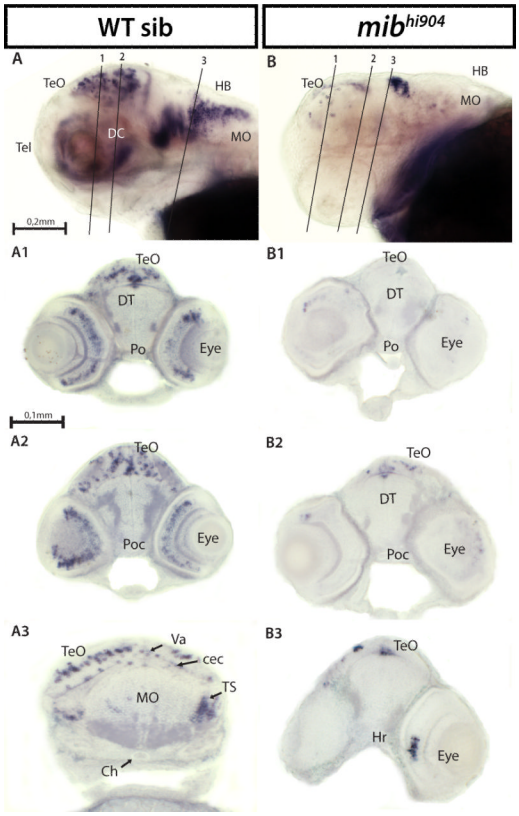

Fig. 6.

dmbx1a mRNA expression. Whole mounts are shown in lateral views (A, B). A1-A3: WISH transversal cryostat sections of a stage 72 hpf WT. B1-B3: WISH transversal cryostat sections of a stage 72 hpf *mib*^{hi904}. Abbreviations (as above): cec, cerebellar commissure; Ch, chorda dorsalis; Poc, postoptic commissure; Va, valvula cerebelli. Scale bars: 0.2 mm (A, B), 0.1 mm (A1–A4, B1-B3).

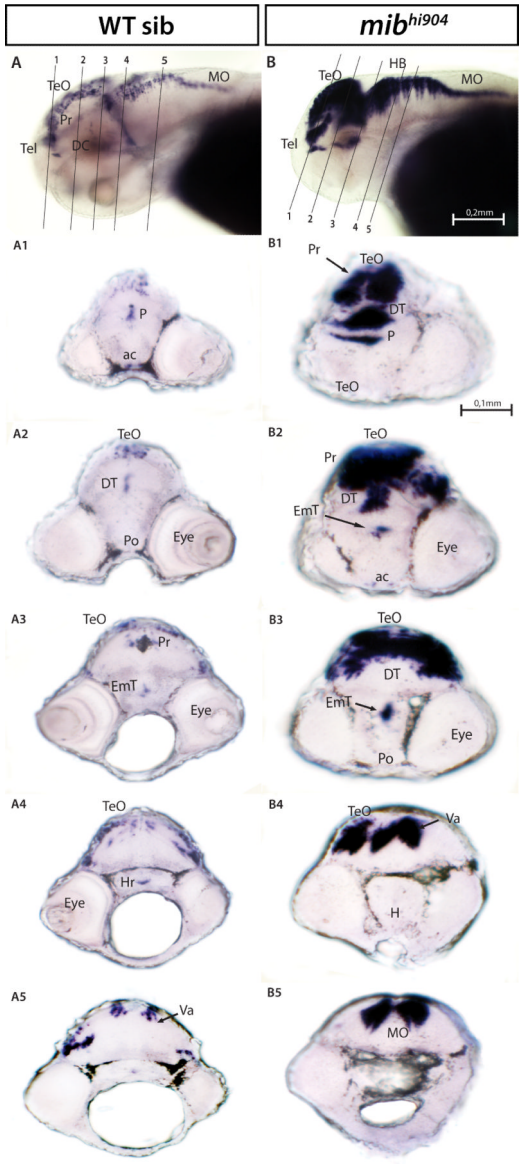

Fig. 7.

dbx1a mRNA expression. Whole mounts are shown in lateral views (A, B). A1-A5: WISH transversal cryostat sections of a stage 72 hpf WT. B1-B5: WISH transversal cryostat sections of a stage 72 hpf *mib*^{hi904}. Abbreviations as above; scale bars: 0.2 mm (A,B) and 0.1 mm (A1–A5, B1-B5).

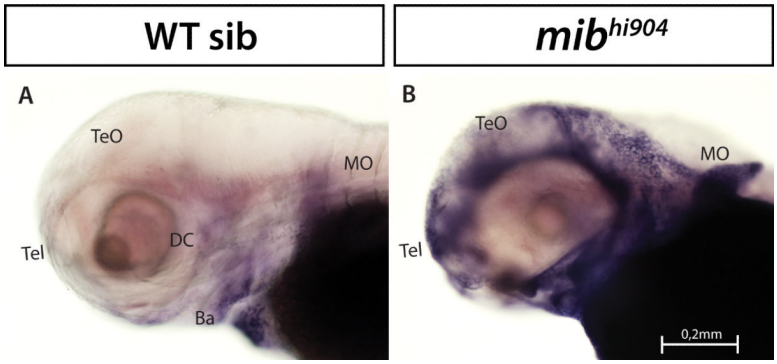

Fig. 8.
plxnd1 mRNA. Whole mounts are shown in lateral views (A, B). Abbreviations as above; scale bars: 0.2 mm (A, B).

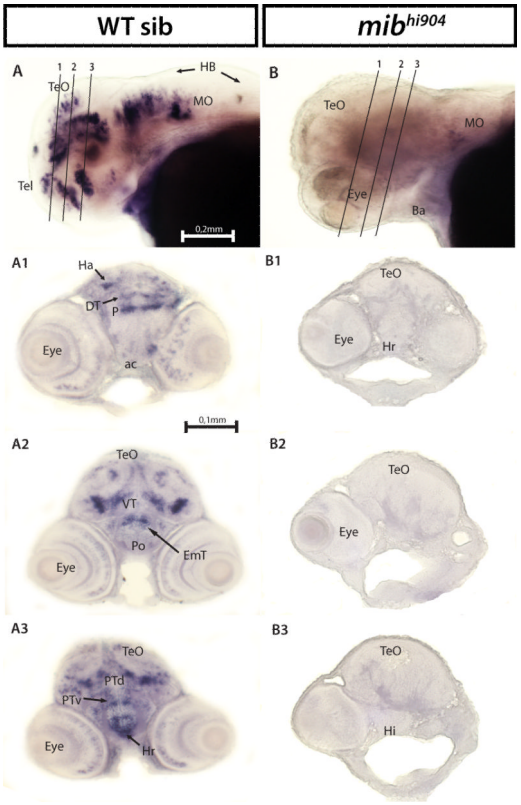

Fig. 9.

nxph1 mRNA. Whole mounts are shown in lateral views (A, B). A1-A3: WISH transversal cryostat sections of a stage 72 hpf WT. B1-B3: WISH transversal cryostat sections of a stage 72 hpf *mib*^{hi904}. Abbreviations (as above): PTd, dorsal part of posterior tuberculum; PTv, ventral part of posterior tuberculum. Scale bars: 0.2 mm (A, B), 0.1 mm (A1-A3, B1-B3).

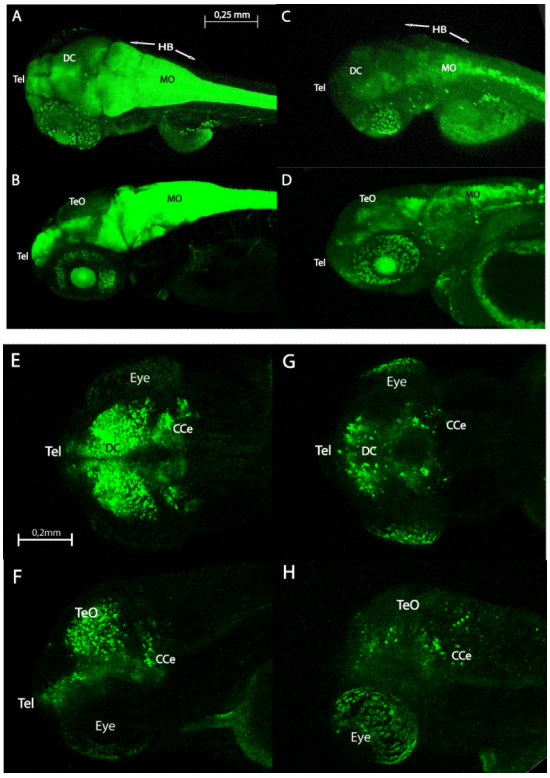

Fig. 10.

Confocal live whole-mount images of Gfap:GFP (upper panel) and Dlx5-6:GFP transgenic zebrafish brain (lower panel) in wild-type (left side) and *mib*^{hi904} mutant (right side) at 3 dpf: dorsal views (A, C, E, G) and lateral views (B, D, F, H). The transgenic line for the GFAP drove expression (shown as green fluorescence) initially in the telencephalon and then in the eye and midbrain. Gfap:GFP is also highly prominent in hindbrain in WT siblings with a weak expression pattern in *mib*^{hi904} mutants. Dlx5-6:GFP in *mib*^{hi904} mutants is reduced with only few cells showing expression in diencephalon, eyes and in the cerebellar region. Images of live zebrafish were obtained using a Leica SP5 confocal scanning fluorescence microscope. Abbreviations as above; scale bars, 0.25 mm (A, B, C, D) and 0.2mm (E, F, G, H).

Table 1

Summary of data extracted from microarrays. Statistical analysis (Ttest, GeneSpring GX 7.3.1) and qPCR analysis (SPSS, two-tailed Student's t test) are shown. GenBank ID, fold changes and P-values.

Gene name	Genbank ID	array-fold	qPCR-fold	p-value (array)	p-value (qPCR)
hairy-related 4.2	BC049296	–3.65	–3.7	0.04	0.003
hairy and enhancer of split 5	AY264404	–2.54	–2.7	0.02	0.001
Basic helix-loop-helix domain containing, class B, 5	BC053312	–5.49	–2.5	0.03	0.001
homeo box A5a	NM_131540	–2.02	–1.2	0.02	0.029
homeobox protein (hoxb5b) gene	NM_131537	–2.07	–1.4	0.05	0.014
diencephalon/mesencephalon homeobox 1a	AY071922	–2.00	–1.8	0 .01	0.001
developing brain homeobox 1a	NM_131158	2.69	1.1	0.03	0 .017
neurexophilin 1	BM072355	–2.21	–1.9	0.05	0.001
plexin D1	BI878456	2.96	1.6	0.04	0.005
glial fibrillary acidic protein	AF506734	–6.27	–3.59	0.009	0.002

Dev Dyn. Author manuscript; available in PMC 2012 August 1.